A High Sensitivity and Low Power Circuit for the Measurement of Abnormal Blood Cell Levels

R. Nagulapalli, K. Hayatleh, S. Barker, A. A. Tammam, F. J. Lidgey and N. Yassine
Oxford Brookes University, Oxford, United Kingdom
khayatleh@brookes.ac.uk

This paper describes a technique to detect blood cell levels based on the time-period modulation of a relaxation oscillator loaded with an Inter Digitated Capacitor (IDC). A digital readout circuit has been proposed to measure the time-period difference between the two oscillators loaded with samples of healthy and (potentially) unhealthy blood. A prototype circuit was designed in 65nm CMOS technology and post-layout simulations shows 15.25aF sensitivity. The total circuit occupies 2184μm^2 silicon area and consumes 216μA from a 1V power supply.

Keywords: time-period discrimination, relaxation oscillator, low power, high sensitivity, abnormal blood cell sensor

1. Introduction:

Due to improved processing capabilities, in terms of flexibility and high storage capacities, electronics-based sensors are getting a lot of attention from the medical field. The fundamental principle behind many of these sensors is that any increase of the contamination density in the cells under test will change the effective dielectric constant (K) [1]. Hence this provides a real-time indication of contamination levels. Harris [2] has given very detailed explanation about the passive electrical properties of biological systems. Biological cell suspensions generally exhibit three major dielectric dispersions in the frequency range of 100-1011Hz. The α-dispersion is seen at audio frequencies and is largely credited to surface admittance, lateral to the membrane surfaces. β-dispersion is centred in the radio-frequency range and is dominated by the Maxwell-Wanger effect at the interface between the suspending medium and the poorly conducting plasma membrane. The γ-dispersion generally occurs at microwave or millimetric-wave frequencies. The main reason for γ-dispersion is the water polarization within the substance [2]. The frequency used in this work is 1.3GHz and hence only γ-dispersion is the dominant dispersion. An approximate effective dielectric constant of a cell suspension is given by Harris [2] and is expressed as (1):

$$\epsilon_{Blood_{test}} = \epsilon_{Blood_{healthy}} + \frac{\delta\epsilon}{1+\left(\frac{f}{f_C}\right)^2} \quad (1)$$

Where $\epsilon_{Blood_{test}}$ is the effective dielectric permittivity of the blood, f_C is the characteristic frequency of the dispersion process, and f is the measurement frequency. The static permittivity change of the blood due to the presence of the contamination can be obtained by making f = 0 in equation (1), which results as follows:

$$\delta\epsilon(\text{cell parameter}) = \frac{9PrC_m}{\epsilon_0} \quad (2)$$

Where r is the radius of the cell and C_m is the membrane capacitance. P (the volume fraction of the cells) is dependent on the concentration of cells N and expressed in [2] as follows:

$$P = \frac{4\Pi r^3 N}{3V_{cap}} \quad (3)$$

Where V_{cap} is the volume of the container. By using equations (1), (2) and (3), the permittivity of the biological cell at microwave frequencies can be written as:

$$\epsilon_{Blood_{test}} = \epsilon_{Blood_{healthy}} + \frac{12\Pi N r^4 C_m}{1+\left(\frac{f}{f_c}\right)^2} \quad (4)$$

From equation (4) above, any substance dielectric constant depends on the concentration of the cells and increases with the contamination density.

A convenient electrical approach to detect the dielectric constant is to measure the capacitance of a parallel plate capacitor with a dielectric of the material of interest, such that capacitance modulation due to that material can be easily detected. This is the basis of the sensor as shown in Fig. 1. Fundamentally, it is a capacitor, with the blood sample forming the dielectric. To prevent resistive elements from the blood sample affecting the results, the capacitor is covered with a very thin insulating membrane. There are several ways to measure capacitance, such as measuring the difference directly with a switched capacitor circuit, or by measuring the frequency of an oscillator loaded with the capacitor. Vehring [3] and Samsingh [4] exploited this method, using an LC-Oscillator to detect the material property change. This is not very useful, however, as there is no means to measure the frequency deviation. Instead, they have measured the frequency of the VCO with and without the material and calculated the frequency change manually. Helmy *et al.,* [5] have demonstrated the method with a PLL rather than with a simple VCO, hence the control voltage of the VCO will give a reasonable estimate of the dielectric change, but unfortunately this is a very power hungry and silicon area inefficient solution. In our previous work [6] we proposed a digital frequency, counter based solution to detect impurity levels in blood. However, in this paper the relationship between capacitance and frequency was not a linear one.

In this paper we are proposing a modification to our previous solution [6] in that the new circuit measures the time-period difference instead of the frequency difference. This new method provides a linear relationship between the capacitance change and the output.

The rest of the paper has been organized as follows. Section 2 describes the basic detection principle. Section 3 describes the Proposed Time-period Detector. Section 4 explains the oscillator implementation. Section 5 explains the time-period detector implementation. Section 6 summarizes the prototype simulation results.

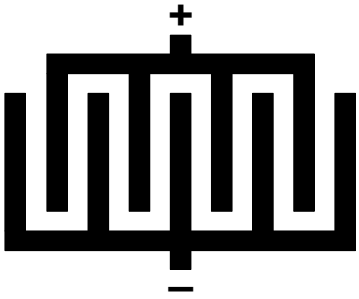

Fig. 1. IDC Based sensor

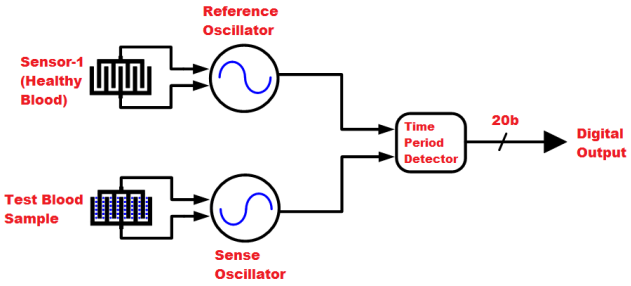

Fig. 2. Abnormal blood cell detection concept

2. Detection Principle:

Fig. 2 shows the detection concept. It is based on our previous work [6], but the detector now detects time-period deviation instead of frequency. One way of detecting a capacitance change is to form an oscillator based on the sensor capacitance, such that change in dielectric constant modulates the capacitance which in turn causes a frequency shift. By comparing this with a reference oscillator frequency, the dielectric constant change can be measured. As shown in Fig. 2, a reference oscillator loaded with sensor-1 oscillates at 1.3GHz, whilst the sensing oscillator based on the sensor-2 (containing the blood test sample) will oscillate at a lower frequency. Hence, by detecting the frequency or time-period difference between the oscillators, we can estimate the capacitance change, and indirectly estimate the volume of abnormal cells. Our previous work [6] we used frequency difference detection. In this paper, we are presenting a time-period based detection to detect change in the capacitance and produce an output with a linear relationship to the level of contamination. This is based on measuring oscillation time-period, which is proportional to capacitance. Therefore increasing (contaminating) cell density will be sensed as a time-period change [1].

Since we are detecting the difference of the time-period of the two similar oscillators, the method is insensitive to process, voltage and temperature (PVT) corner variations. In principle, there are three types of oscillators: Ring, Inductor-Capacitance (LC) and Relaxation oscillators. Due to the size and matched oscillator requirement, the LC approach hasn't been adopted, since multiple inductors, on the same chip, could lead to inductive coupling and injection pulling which could affect the performance. Razavi *et al.* [7][11] used an LC oscillator, but they ensured a considerable distance between the two inductors, so that any coupling was negligible. Unfortunately, this is a very inefficient approach, regarding silicon area. Another problem with the LC oscillator is that the time-period is dependent on the square root of the capacitance (from equation 5). This means a 4% change in capacitance will cause a 2% change in the time-period. The ring oscillator is tiny compared with other oscillators, but it needs multiple sensor capacitors as every delay stage requires capacitance. It is very difficult to accommodate several similar sensors and the silicon area would be comparatively large. The relaxation oscillator occupies a very small area compared to other oscillators, and it works with a single capacitance, thus making it ideal for this application. The time-period for the Relaxation and Ring oscillators depends directly on the capacitance, from equation 6, hence a 4% capacitance change will result in a 4% time-period change, therefore there is a greater sensitivity to capacitance variation.

$$T_{LC} = 2\Pi\sqrt{LC} \quad \text{Hence} \quad \frac{\delta T_{LC}}{T_{LC}} = 0.5\frac{\delta C}{C} \tag{5}$$

$$T_{RC} = 2\Pi RC \ \text{Hence} \quad \frac{\delta T_{RC}}{T_{RC}} = \frac{\delta C}{C} \tag{6}$$

From equation (6) time-period is proportional to capacitance, hence the time-period detection would yield a linear relationship between the capacitance and the detector output.

3. Proposed Time-period Detector (TPD):

Our previous frequency-based work [6][12] was based on a detection concept depicted in Fig. 3(a). The reference counter operates on the reference frequency F_{Ref} (generated from the oscillator loaded by healthy blood) and the sense counter runs on sensor frequency F_{Sen} (generated from the oscillator loaded by the test blood sample). The reference counter reaches the max count/code (all 1s) in the 2nd reference cycle and releases a freeze signal as shown in Fig. 3(b). The sensor counter state lags the reference counter because it is running at a slower frequency and stops counting when it receives the freeze signal, hence the output state will get locked. The time taken by the reference counter to reach the freeze state (T_{Frz}) is given by equation 7 and the sensor counter locked state (in decimal equivalent) can be expressed as shown by equation 8. This shows that counter output state is proportional to the sense oscillator frequency, hence it is inversely proportional to the sense capacitance. This means that the slope of the output code vs capacitance curve will decrease with an increase in the capacitance. Hence the sensitivity reduces with increases in capacitance, which is not desirable from a sensor, as a linear relation is always more desirable for constant sensitivity. Fig. 3(a) shows pictorial representation of how the digital circuit will be configured and 3(b) shows how the counters will be frozen.

$$T_{Frz} = \frac{2^N}{F_{REF}} \tag{7}$$

$$D_{OUT} = 2^N \frac{F_{Sen}}{F_{Ref}} \tag{8}$$

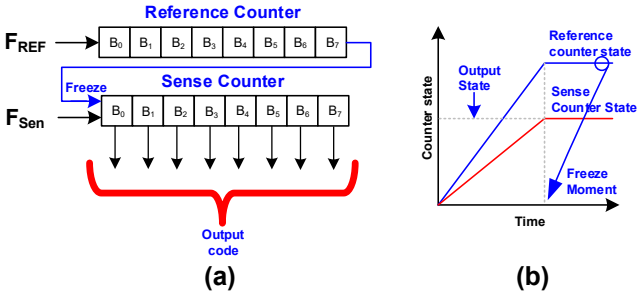

Fig. 3. (a) Detection concept [6], (b) Counter states w.r.t time

To solve this non-linear sensitivity problem, a modification to the existing technique is proposed, based on time-period detection instead of frequency. Fig. 4 shows the proposed concept, which relies on freezing the sense counter and locking the reference counter at this point. The output code is read as the sensor output. The problem here is that since the reference counter is running on a high frequency clock, it may overflow and start recounting from the initial state. To avoid this, the reference counter should always contain a higher number of bits than the sense counter. This is achieved by estimating the maximum possible frequency difference between the two clocks.

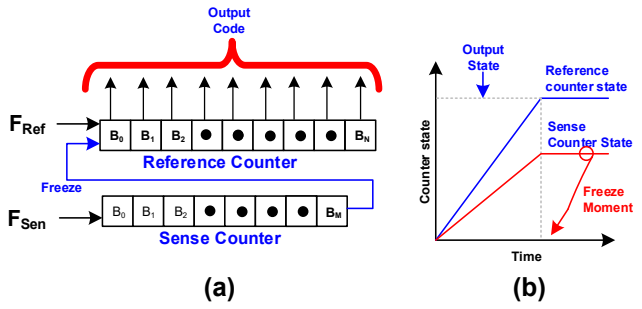

Fig. 4. Proposed Detection concept (a) Circuit (b) Counter states

Assuming the reference and sense counters have bit lengths N and M respectively, the sense counter freezing time can be expressed as:

$$T_{Frz} = \frac{2^M}{F_{Sen}} \tag{9}$$

The reference counter state at the T_{frz} instant is expressed as:

$$D_{Out} = 2^N \frac{F_{Ref}}{F_{Sen}} = 2^N \frac{T_{Sen}}{T_{Ref}} \tag{10}$$

Equation (10) reveals that output code is proportional to T_{Sen} from equation (9). This shows that the output code is proportional to the sensor capacitance. The relationship between the sensor capacitance and the output is linear with a constant slope, hence the sensitivity for any level of cell abnormality in the blood is constant, whereas the existing sensor sensitivity is a function of the level of cell abnormality[13].

4. Oscillator Implementation details:

Fig. 5 shows the circuit diagram of an implemented oscillator circuit [9]. In our previous work [6] the only way to tune the frequency was to change the charging resistor (to make the semiconductor implementation process cheaper, we are not considering varactors in this design)[14]. In Fig. 5 the bias current (I_B) can be programmed to tune the frequency to a desired value. Though tuning the VCO is not the major goal here, the reference frequency needs to be as high as possible to improve the sensitivity. The relaxation oscillator presented works as follows. When the output node is at a logic high state, the capacitor C_S (Fig. 5(a)) discharges with the slope given by I_2/C_S. This occurs as soon as node X voltage crosses the low threshold voltage (V_L) of the comparators, and the SR latch will flip the output state. Hence the output state is low. Due to the low logic state, C_S charges with the slope given by I_1/C_S as shown in Fig. 5(b) and as soon as this reaches a high threshold voltage (V_H) SR latch will flip the output state, and the oscillation process thus continues. The main goal of the comparator implementation [8][15], as shown in fig. 6, is to minimize the offset and operating power.

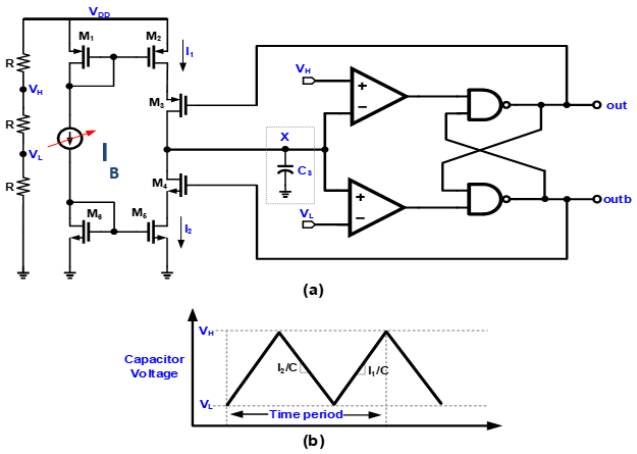

Fig. 5. (a) Relaxation Oscillator Schematic (b) Voltage across Capacitor

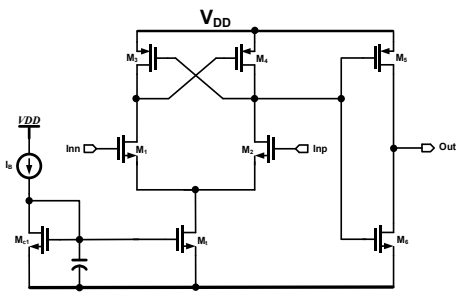

Fig.6. Regenerative Comparator schematic.

The frequency of oscillation can be expressed as follows.

$$F_{OSC} = \frac{1}{C_S(V_H - V_L)\left(\frac{1}{I_1}+\frac{1}{I_2}\right)} \tag{11}$$

By substituting equation (11) into equation (10), the reference sensor state or sensor output can be expressed as follows:

$$D_{out} = 2^N \frac{C_{Bloodtestsample}}{C_{Healthyblood}} \tag{12}$$

This shows there is a linear relationship between the test sample capacitance and the output.

The oscillator frequency impacts the power consumption and sensitivity of the sensor in different ways. A higher oscillation frequency results in improved sensitivity but consumes more power and vice versa. In 65nm CMOS technology, designing an oscillator with a frequency greater than 1.3GHz will exponentially increase power consumption. Hence the sensor is designed to operate at this frequency.

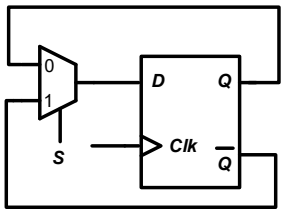

Fig. 7. Loadable flip-flop design.

5. TPD Implementation details:

Fig. 7 shows a loadable flip-flop, which behaves like a flip-flop when the control signal (S) is high and behaves like a memory element when control signal is low [6]. This is used in the design of both the reference and sense counters. This allows us to freeze the state using the control signal S (Fig. 7). The gate level implementation of the proposed time-period detector (TPD) is shown in Fig. 8. The sense and reference counter are standard ripple counters. When clock signals are applied to the detector of the sense counter, it eventually reaches the full stage or freezing point (all outputs are in a logic high state). This freezing point will be detected by a 16 input NAND gate which will produce logic ‘high’ freeze output when the sense counter reaches the full state, which also freezes the reference counter. As explained in section-3, the reference counter needs to have more bits than the sensor counter to avoid the danger of recounting. The difference in the number of bits depends on the level of capacitance change due to the impurities, compared to sensor-1. If the capacitance changes by a factor of 4, then the reference counter should be able to handle 4 times the frequency, hence it needs at least 2 bits more. In the present design, we used 4 extra bits (a 16 bit sensor counter and a 20 bit reference counter).

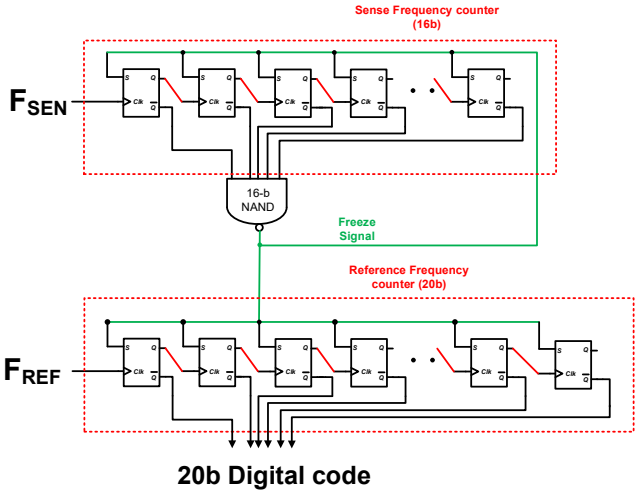

Fig. 8. Time-Period detector Schematic

6. Simulation results:

A transistor level Sensor has been developed in 1 poly and 8-metal 65nm CMOS TSMC technology and post-layout simulations has been carried out. At room temperature the sensor consumes 216uA current from a 1.2V power supply. Fig. 9 shows the relationship between the relaxation oscillator frequency and the capacitance. Sensor-1 has been loaded with 1pF (to represent the healthy blood capacitance) and the reference oscillator frequency is 1300MHz. Sensor-2 has been loaded with a variable capacitance between 1pF to 4pF, which represents abnormal blood. For example, when sensor-2 is loaded with 1.4pF capacitance, then the sense oscillator oscillates at 928MHz (1.0775ns time-period) [16]. To reach the freezing state it must count 216 cycles, hence the counter must count for 70.615µs. Since both counters will freeze at the same time, and reference oscillator time-period is 0.769ns, hence the reference counter counts 91803 cycles. By this time, the number of cycles exactly represents the capacitance and the level of abnormal cells. Fig. 10 is a representation of the sensor output. The simulation for the different abnormal blood cell levels was done by sweeping the sensor-2 capacitance from 1pF to 4pF. Fig. 11 shows the sensor output (decimal equivalent of a 20-bit output) versus the capacitance, as explained in the section-3. The sensor output is linearly increasing with the capacitance, hence the sensitivity (slope) is near constant irrespective of the level of abnormal cell levels. For an almost 3pF change in the sense capacitance (meaning x-axis variation from 1pF to 4pF), the output of the sensor is changed by 196608 LSBs. Therefore, there is a 15.25aF capacitance change required to update the output state by 1 LSB, hence 15.25aF is the sensitivity of the proposed sensor. Sensitivity is generally a ratio of two quantities. Although it is defined here as capacitance per unit LSB, for simplicity, we are quoting it in terms of the capacitance itself. Fig. 12 shows the layout of the entire detection system. It is a pad limited circuit and occupies 0.3825mm2 silicon area [17]. Pads named as B0-B19 represent the output signals from the reference counter [10]. One way to reduce the area could be by using a serial interface protocol like SPI or I^2C. These would reduce the 20 output pads to only two (clock and data) but requires integrating the associated circuitry involved with the protocol. Table-I compares the performance of this sensor with other state of art designs.

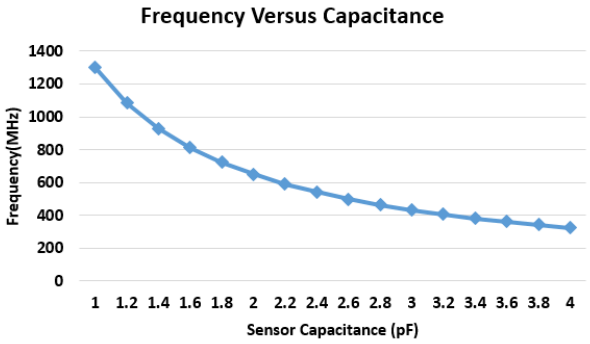

Fig. 9. Relaxation oscillator Frequency Characteristics

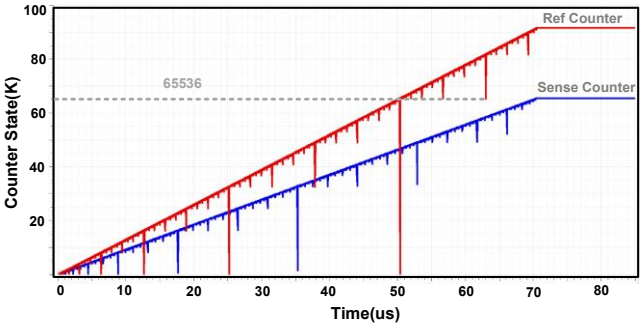

Fig. 10. Sensor detection waveforms for 1.4pF sensor capcitance.

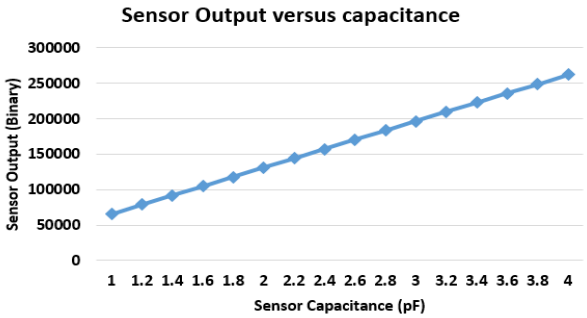

Fig. 11. Output of the sensor versus the capacitance.

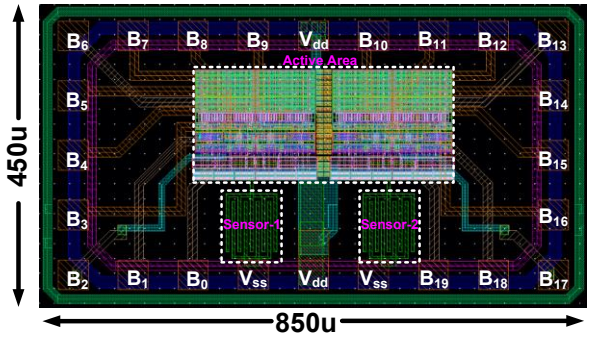

Fig. 12. Layout of the Sensor.

Table-I: comparison of sensor performance with other state of art designs.

Parameter	This Work	[5]	[6]
Detection Method	Time period	Frequency	Frequency
VCO Type	Relaxation	LC	Relaxation
Sensetivity	15.25aF	Not reported	210aF
Power consumption (mW)	0.216	16.5	0.42
CMOS Technology(nm)	65	90	65
Area (mm2)	0.3825	6.25	0.2925

7. Conclusion:

A time-period modulation-based blood cell abnormality sensor has been proposed with a 20-bit digital readout. This sensor can detect a minimum of 15.25aF capacitance change and has very low power consumption. A transistor level circuit has been implemented and post layout simulations have been carried out. The circuit consumes 216uA from a 1V power supply, at room temperature.

8. References

1. Nuutinen, J., Ika¨heimo, R., & Lahtinen, T. (2004). Validation of a new dielectric device to assess changes of tissue water in skin and subcutaneous fat. Physiological Measurement, 25(2), 447–454.
2. Harris, C., & Dell, D. (1983). The radio frequency dielectric properties of yeast cells measured with rapid automated frequency domain dielectric spectrometer. Bio-electrochemistry and Bioenergetics, 11, 14–28.
3. R. Nagulapalli, K. Hayatleh, S. Barker, S. Zourob, N. Yassine and S. Sridevi, "A PVT insensitive programmable amplifier for biomedical applications," *2017 International conference on Microelectronic Devices, Circuits and Systems (ICMDCS)*, Vellore, 2017, pp. 1-5.
4. V. R. Samsingh *et al*., "Characterization of Delamination in Fiber-Reinforced Epoxy-Based PCB Laminates, Using an EBG-Enhanced Planar Microwave Sensor," in *IEEE Transactions on Components, Packaging and Manufacturing Technology*, vol. 7, no. 10, pp. 1739-1746, Oct. 2017.
5. Helmy, A., Jeon, H.-J., Lo, Y.-C., Larsson, A., Kulkarni, R., Kim, J., et al. (2012). A self-sustained CMOS microwave chemical sensor using a frequency synthesizer. IEEE Journal of Solid-State Circuits, 47(10), 2467–2483.
6. Nagulapalli, R., Hayatleh, K., Barker, S. et al. Analog Integr Circ Sig Process (2017) 92: 437. https://doi.org/10.1007/s10470-017-1008-1
7. R. Nagulapalli, S. Zourob, K. Hayatleh, N. Yassine, S. Barker and A. Venkatareddy, "A compact high gain opamp for Bio-medical appli-cations in 45nm CMOStechnology," *2017 2nd IEEE International Conference on Recent Trends in Electronics, Information & Communication Technology (RTEICT)*, Bangalore, 2017, pp. 231-235.
8. P. E. Allen and D. R. Holberg, CMOS Analog Circuit Design, Oxford University Press, 2002.
9. K. Tsubaki, T. Hirose, Y. Osaki, S. Shiga, N. Kuroki, and M. Numa, "A 6. 66-kHz, 940-nW, 56ppm/°C Fully On-chip PVT Variation Tolerant CMOS Relaxation Oscillator," 19th IEEE International Conference on Electronics, Circuits, and Systems (ICECS), pp. 97-100, 2012.
10. R. Nagulapalli, K. Hayatleh, S. Barker, S. Zourob, N. Yassine and S. Sridevi, "A bio-medical compatible self bias opamp in 45nm CMOS technology," *2017 International conference on Microelectronic Devices, Circuits and Systems (ICMDCS)*, Vellore, 2017, pp. 1-4.
11. R. Nagulapalli, K. Hayatleh, S. Barker, S. Zourob and A. Venkatareddy, "A novel current reference in 45nm cmos technology," *2017 Second International Conference on Electrical, Computer and Communication Technologies (ICECCT)*, Coimbatore, 2017, pp. 1-4.
12. E. E. Krommenhoek *et al*., "Monitoring of yeast cell concentration using a micromachined impedance sensor," *The 13th International Conference on Solid-State Sensors, Actuators and Microsystems, 2005. Digest of Technical Papers. TRANSDUCERS '05.*, Seoul, South Korea, 2005, pp. 283-286 Vol. 1.
13. R. Nagulapalli, K. Hayatleh, S. Barker, S. Zourob, N. Yassine and B. N. K. Reddy, "A Technique to Reduce the Capacitor Size in Two Stage Miller Compensated Opamp.," *2018 9th International Conference on Computing, Communication and Networking Technologies (ICCCNT)*, Bangalore, 2018, pp. 1-4.
14. Jiangfeng Wu, G. K. Fedder and L. R. Carley, "A low-noise low-offset capacitive sensing amplifier for a 50-/spl mu/g//spl radic/Hz monolithic CMOS MEMS accelerometer," in *IEEE Journal of Solid-State Circuits*, vol. 39, no. 5, pp. 722-730, May 2004.
15. T. H. Lee The Design of CMOS Radio-Frequency Integrated Circuits United Kingdom:Cambridge University Press 1998.
16. A. Sodagar G. Perlin Y. Yao K. Najafi K. Wise "An implantable 64-channel wireless microsystem for single-unit neural recording" IEEE J. Solid-State Circuits vol. 44 pp. 2591-2604 Sep. 2009.
17. R. Nagulapalli, K. Hayatleh, S. Barker, S. Zourob, N. Yassine and S. Sridevi, "A Microwatt Low Voltage Bandgap Reference for Bio-medical Applications," *2017 International Conference on Recent Advances in Electronics and Communication Technology (ICRAECT)*, Bangalore, 2017, pp. 61-65.